

JOINT ESTIMATION OF AMPLITUDE, DIRECTION OF ARRIVAL AND RANGE OF NEAR FIELD SOURCES USING MEMETIC COMPUTING

F. Zaman^{1, *}, I. M. Qureshi¹, A. Naveed², and Z. U. Khan¹

¹Department of Electronic Engineering, IIU, H-10, Islamabad, Pakistan

²School of Engineering & Applied Science, ISRA University, Islamabad, Pakistan

Abstract—In this paper, we propose a method based on evolutionary computations for joint estimation of amplitude, Direction of Arrival and range of near field sources. We use memetic computing in which the problem starts with a global optimizer and ends up with a local optimizer for fine tuning. For this, we use Genetic algorithm and Simulated annealing as a global optimizer while Interior Point Algorithm as a rapid local optimizer. We set up Mean Square Error as a fitness evaluation function which defines an error between actual and estimated signal. This fitness function is optimum and is derived from Maximum likelihood principle. It requires only single snapshot to converge and does not require any permutations to link it with the angles found in the previous snapshot as in some other methods. The efficiency and reliability of the proposed scheme is tested on the basis of Monte-Carlo simulations and its inclusive statistical analysis.

1. INTRODUCTION

Estimating the parameters, especially Direction of Arrival (DOA) of multiple electromagnetic waves is an important issue and is directly applicable to radar, radio astronomy, mobile communication and smart antennas [1, 2]. It is relatively easy to estimate the DOA of waves impinging from far field sources because all the wave-fronts are assumed to be plane waves. Many classical algorithms exist for such case like MUSIC, ESPRIT, Maximum Likelihood (ML) and Capon [3]. The situation becomes more complicated when the sources

Received 28 May 2012, Accepted 23 July 2012, Scheduled 24 July 2012

* Corresponding author: Fawad Zaman (fawad.phdee31@iiu.edu.pk).

are in the Fresnel zone (Near field) of array aperture. In such situations, the wave-front is no longer planar but is spherical and the source location cannot be solely found by simply estimating the angle. In this case, along with the angle, we also need to estimate correctly the range of sources [4]. Hence, the techniques developed for the estimation of far field sources cannot be applied directly to estimate the DOA of near field sources. Near field situation can occur in many practical situations such as, electronic surveillance, seismic exploration, ultrasonic imaging, under water source localization and speech enhancement with microphone arrays [5]. For joint estimation of ranges and DOA, Maximum Likelihood (ML) method was proposed first [6]. Later on an effort was made by using least squares ESPRIT like algorithm based on fourth order cummulants but this is computationally heavy [7]. In [8], a weighted linear prediction method was proposed which needs additional computation to solve pairing problem in the case of multiple sources but this can result in inaccurate pairing at low Signal-to Noise (SNR) when arrival angles are closely spaced.

In todays developments, no one can deny the significance of evolutionary computational techniques such as Genetic algorithm (GA), Particle Swarm Optimization (PSO), Genetic programming (GP) and Differential evolution (DE) etc.. These techniques are based on principle of biological evolution such as genetic inheritance and natural selection. Among these evolutionary techniques, GA received extra attention due to its simplicity in understanding, ease in implementation and more importantly having less probability of getting stuck in the presence of local minima. GA is being successfully widely applied to a mixture of problems ranging from handy applications in industry and commerce to leading-edge scientific research. In many problems the efficiency and reliability of GA significantly improves when it is hybridized with any other efficient evolutionary computational technique such as Pattern Search (PS), Active Set (AS) and Interior Point algorithm (IPA) etc. [9–11]. In [11], the amplitude and DOA of far field sources impinging on L-type array are jointly estimated and the performance of GA, PS and Simulated Annealing (SA) is compared with the hybrid approach GA-PS and SA-PS. For all these schemes Mean Square Error (MSE) is used as a fitness evaluation function. In [12], the same MSE is used as a fitness evaluation function with PSO for DOA estimation of far field sources impinging on uniform linear array (ULA).

In this paper, we propose a method based on memetic computing for joint estimation of amplitude, DOA and range of near field sources. We use GA, IPA, SA, GA-IPA and SA-IPA in which GA and SA are

used as global optimizers while IPA is used as a rapid local optimizer for further fine-tuning. For this, we used MSE as a fitness evaluation function which defines an error between actual and estimated signals. This fitness function is optimum and is derived from ML. It has the advantage of linking automatically the DOA estimated in the previous snapshot to a current estimated DOA which is the main issue in multiple targets tracking system [13]. Moreover, this fitness function is real in nature, avoids any ambiguity between the angles that are supplement to each other, requires only single snapshot to converge and provides fairly good results even in the presence of low Signal to Noise ratio (SNR). The efficiency and reliability of the proposed approach is tested on the basis of large number of Monte-Carlo simulations and its statistical analysis.

This paper is organized as follows: In Section 2, we have given the data model, in Section 3, we discussed the proposed methodology while Sections 4 and 5, are devoted for results and future work direction respectively.

2. DATA MODEL

Consider P near field sources impinging on a passive uniform linear array. This linear array consists of $N = 2N_x$ sensors and having the same inter-element spacing between the two consecutive elements as shown in Fig. 1 [14].

We have assumed that the impinging wave is narrow band, zero mean and having unit variance σ_i^2 . For this, our signal model on l th sensor in the array can be written as,

$$x_l = \sum_{i=1}^P s_i \exp(j(\alpha_i l + \beta_i l^2)) + \eta_l \tag{1}$$

for $l = -N_x + 1, \dots, 0, 1, \dots, N_x$, where $l = 0$ is the phase reference

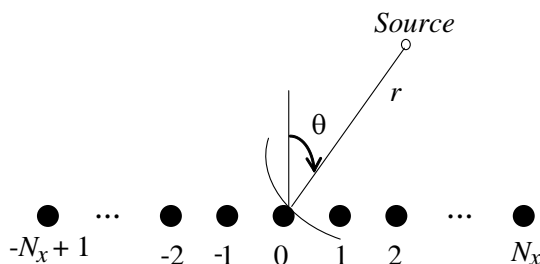


Figure 1. Array geometry.

point of our co-ordinate system. The parameters α_i and β_i in (1) are the function of elevation angle θ_i and range r_i respectively of the i th source. Mathematically it can be expressed as follow,

$$\alpha_i = \frac{-2\pi d}{\lambda} \sin(\theta_i)$$

and

$$\beta_i = \frac{\pi d^2}{\lambda r_i} \cos^2(\theta_i)$$

In matrix-Vector form (1) can be written as

$$\mathbf{x} = \mathbf{A}\mathbf{s} + \boldsymbol{\eta} \quad (2)$$

where

$$\begin{aligned} \mathbf{x} &= [x_{-N_x+1}, \dots, x_o \dots x_{N_x}]^T \\ \mathbf{s} &= [s_1, s_2, \dots, s_P]^T \\ \boldsymbol{\eta} &= [\eta_{-N_x+1}, \dots, \eta_o \dots \eta_{N_x}]^T \\ \mathbf{A} &= [\mathbf{a}_1, \mathbf{a}_2, \dots, \mathbf{a}_P] \end{aligned}$$

where $\mathbf{a}_i(\theta_i, r_i) = [\exp(j(-N_x+1)\alpha_i + j(-N_x+1)^2\beta_i), \dots, \exp(j(-\alpha_i + \beta_i)), 1, \exp(j(\alpha_i + \beta_i)), \dots, \exp(j(N_x\alpha_i + N_x^2\beta_i))]^T$ is the steering vector. The goal of this paper is to estimate jointly the unknown parameters, i.e., the amplitude (s_i), elevation angle (θ_i) and range (r_i) of the waves for $i = 1, 2, \dots, P$ as given by (1).

3. PROPOSED METHODOLOGIES

In this section, flow diagram, brief introduction and parameter setting of GA, IPA, SA, GA-IPA and SA-IPA is given for joint estimation of amplitude, DOA and range of near field sources.

The Interior Point Algorithm (IPA), which is also called barrier method, was invented by John von Neumann [15]. It is a certain class of algorithms used for linear and non-linear optimization problems. It reaches the optimum solution of the problem by going through the feasible region of the problem rather than its surrounding [16].

Simulated Annealing (SA) technique is used for local and global optimization problem. The main purpose of SA algorithm is to proficiently locate the candidate solution in fixed amount of time. SA has already got application in many engineering problems such as 3-D face recognition problem, unit commitment problem and transmission network expansion planning problem etc. [17, 18].

Genetic Algorithm (GA) belongs to a large family of evolutionary computing which was first discovered by John. H. Holland in 1970 and

is considered to be more reliable and efficient algorithm than any other evolutionary technique. Due to ease in implementation, less probable to get stuck in the presence of local minima, it has been widely used in the field of soft computing, communication and especially in array signal processing [19, 20].

The flow chart of GA and hybrid GA-IPA is shown in Fig. 2 while the steps are given as follows.

Step 1 Initialization: Generate M number of particles at random where each particle (chromosome) consists of unknown (genes), i.e., amplitude, DOA and range. The length of each particle (chromosome) is $3 \times P$ where P is number of sources. Mathematically, it can be written as

$$\begin{aligned} \mathbf{b}_i &= [s_{i,1}, \dots, s_{i,P}, \theta_{i,P+1}, \dots, \theta_{i,2P}, r_{i,2P+1}, \dots, r_{i,3P}] \\ &= [b_{i1}, \dots, b_{iP}, b_{i,P+1}, \dots, b_{i,2P}, b_{i,2P+1}, \dots, b_{i,3P}] \end{aligned}$$

where $s_{ij} \in R : L_s \leq s_{ij} \leq H_s, \forall i = 1, 2, \dots, M, j = 1, 2, \dots, P$, where L_s and H_s are the lowest and highest possible limits of the signal amplitudes. Similarly, $\theta_{ij} \in R : 0 \leq \theta_{ij} \leq \pi, \forall i = 1, 2, \dots, M, j = P + 1, P + 2, \dots, 2P$, and $r_{ij} \in R : L_r \leq r_{ij} \leq H_r, \forall i = 1, 2, \dots, M, j = 2P + 1, 2P + 2, \dots, 3P$, where L_r and H_r are the lowest and highest possible limits of the source ranges.

Step 2 Fitness Evaluation: Calculate the fitness of each chromosome by using the following fitness function

$$D(i) = (1/M) \sum_{l=1}^M |x_l - \hat{x}_l^k|^2 \tag{3}$$

This fitness function is derived from the Maximum likelihood, i.e.,

$$p(X/s, \theta, r) = \frac{1}{(2\pi\sigma_n^2)^N} \exp \left(- \left(\frac{1}{2\pi\sigma_n^2} \left\| X - \hat{A}\hat{s} \right\|^2 \right) \right)$$

where the probability of X is to be maximized and conditioned on $\bar{s}, \bar{\theta}, \bar{r}$. It is very obvious that to maximize $p(X/s, \theta, r)$, we need to minimize $\left\| X - \hat{A}\hat{s} \right\|^2$ which is actually our MSE (fitness function).

In (3) x_l is given by (1) while \hat{x}_l^k is given by

$$\hat{x}_l^k = \sum_{k=1}^P b_k \exp \left(j \left(\hat{\omega}_k l + \hat{\phi}_k l^2 \right) \right)$$

where

$$\begin{aligned} \hat{\omega}_k &= \frac{-2\pi d}{\lambda} \sin \left(\hat{b}_{P+k} \right) \\ \hat{\phi}_k &= \frac{\pi d^2}{\lambda r_{b,2P+k}} \cos^2 \left(\hat{b}_{P+k} \right) \quad \text{For } k = 1, 2, \dots, P. \end{aligned}$$

Step 3 Termination Criteria: The termination criteria of the algorithm are made on the following results achieved, if the pre-defined fitness value is achieved, i.e., 10^{-12} OR if the maximum numbers of cycles have reached.

Step 4 Reproduction: Use the operators of Elitism, crossover, and Mutation selection as shown in Tables 1 & 2, to mimic the new population.

Step 5 Refinement: IPA algorithm is used for further refinement of the results (Call FMINCON Function of MATLAB). The best individual of GA and SA has been set as a preliminary point to IPA algorithm.

Step 6 Storage: Store the global best of this cycle and repeat the steps 2 to 5 for sufficient number of independent runs, which will ultimately be used for better statistical analysis.

4. SIMULATION AND RESULTS

In this section, the accuracy and reliability of GA, IPA, SA, GA-IPA, and SA-IPA are discussed for joint estimation of amplitudes, DOAs, and Ranges of near field sources. A uniform aperture array having $N = 2N_x$ sensors is used in which the inter-element spacing “ d ” between the two consecutive sensors is same, i.e., $\lambda/4$. MSE is setup as a fitness evaluation function which is given by (3). Different cases are discussed on the basis of different number of sources and different number of sensors in the array. The proximity in terms of

Table 1. Parameters settings for GA and IPA.

GA		IPA	
Parameters	Settings	Parameters	Setting
Population size	240	Chromosome size	30
No of Generation	1000	Sub problem algorithm	1d1 factorization
Migration Direction	Both Way	Maximum perturbation	0.1
Crossover fraction	0.2	Minimum perturbation	$1e^{-8}$
Crossover	Heuristic	Scaling	Objective & Constraint
Function Tolerance	10–12	Hessian	BFGS
Initial range	[0–1]	Derivative type	Central difference
Scaling function	Rank	Penalty factor	100
Selection	Stochastic uniform	Maximum function evaluation	50000
Elite count	2	Maximum Iteration	1000
Mutation function	Adaptive feasible	X Tolerance	10–15

Table 2. Parameters settings for SA.

SA	
Parameters	Settings
Annealing Function	Fast
Reannealing interval	100
Temperature update function	Exponential temperature update
Initial temperature	100
Data type	Double
Function Tolerance	10–12
Max iteration	1000
Max function evaluations	3000* number of variables

angular separation, distance and signal level is also examined for GA-IPA. All the values of DOA are taken in radians while the values of ranges are taken as a multiple of wavelength (λ). A MATLAB built-in toolbox “optimization of population” based algorithm is used with the setting shown in Tables 1, 2 and a MATLAB version 7.8.0.347. Throughout the simulations, only a single snapshot is used and each result is averaged over 50 independent runs.

4.1. Case I

In this case, the accuracy of all techniques is discussed for two sources and eight sensors in the (ULA). The amplitudes, DOAs and ranges of these two sources are denoted by $s_1, s_2, \theta_1, \theta_2, r_1, r_2$ respectively. Actual values are taken as $s_1 = 1, s_2 = 2, \theta_1 = 0.6981$ (rad), $\theta_2 = 1.2217$ (rad), $r_1 = 3\lambda, r_2 = 4\lambda$ where as s_1, θ_1, r_1 , correspond to the first source while s_2, θ_2, r_2 , correspond to the second source. As shown in Table 3, all the five schemes produced fairly good estimates, however, among these techniques, the hybrid GA-IPA gives better results. The second and third best results is given by GA and IPA respectively for the same said problem.

Now, the reliability of all schemes in terms of their MSE and convergence rate (reliability) is discussed for increasing number of sensors in the array. By convergence, we imply the percentage of total number of times, a particular technique achieves the actual values under the same condition. For this purpose, 10^{-2} is used as a threshold MSE value. Initially, the array consists of four sensors for which the GA converges 90% with MSE 10^{-5} as shown in Table 4. The convergence and MSE of GA improve when it is hybridized with IPA which has

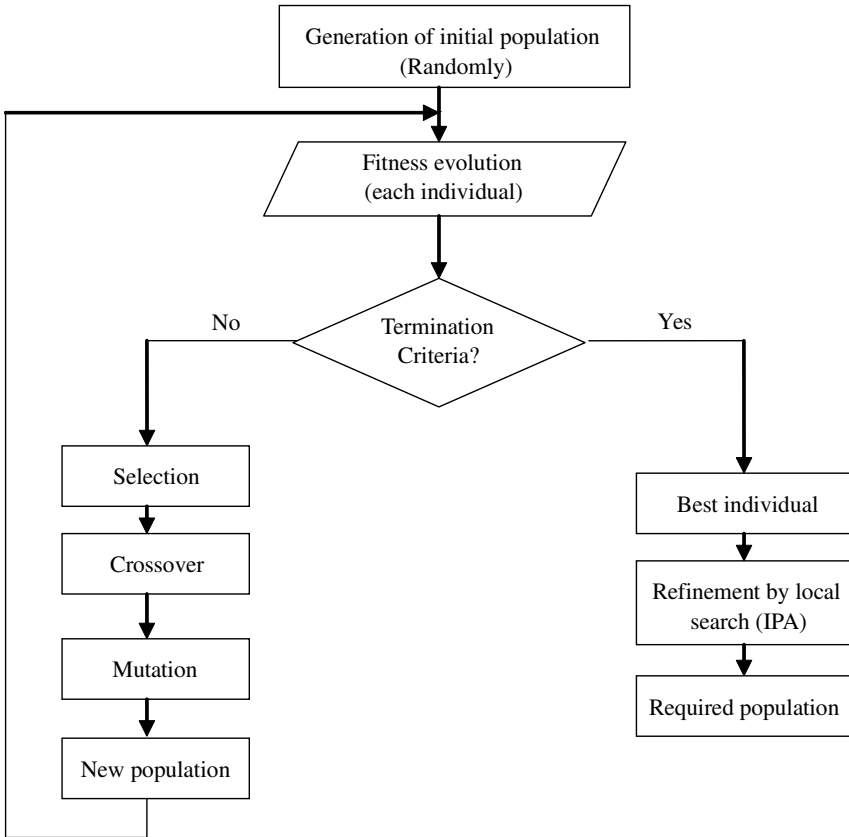


Figure 2. Generic flow diagram of intelligent hybrid computing

Table 3. Amplitude, DOA and range of two sources.

Scheme	s_1	s_2	θ_1 (rad)	θ_2 (rad)	$r_1\lambda$	$r_2\lambda$
Actual values	1.0000	2.0000	0.6981	1.2217	0.3000	4.0000
GA	1.0024	2.0026	0.7006	1.2243	0.3025	4.0027
IPA	1.0088	2.0089	0.7069	1.2306	0.3088	4.0089
GA-IPA	1.0015	2.0015	0.6996	1.2232	0.3015	4.0015
SA	1.0206	2.0205	0.7187	1.2423	0.3206	4.0207
SA-IPA	1.0104	2.0105	0.7089	1.2326	0.3104	4.0106

Table 4. MSE and % convergence of two sources for different number of sensors.

No. of Elements	Scheme	MSE	% Convergence	No. of Elements	Scheme	MSE	% Convergence
4	GA	10^{-5}	90	8	GA	10^{-7}	92
	IPA	10^{-3}	40		IPA	10^{-4}	45
	GA-IPA	10^{-6}	93		GA-IPA	10^{-8}	95
	SA	10^{-3}	10		SA	10^{-4}	13
	SA-IPA	10^{-4}	30		SA-IPA	10^{-5}	34
6	GA	10^{-6}	92	10	GA	10^{-8}	93
	IPA	10^{-3}	42		IPA	10^{-4}	48
	GA-IPA	10^{-7}	94		GA-IPA	10^{-9}	96
	SA	10^{-3}	11		SA	10^{-4}	14
	SA-IPA	10^{-4}	32		SA-IPA	10^{-6}	35

Table 5. Amplitude, DOA and range of three sources.

Scheme	s_1	s_2	s_3	θ_1 (rad)	θ_2 (rad)	θ_3 (rad)	r_1 (λ)	r_2 (λ)	r_3 (λ)
Actual	1.0000	2.0000	3.0000	0.8727	1.3963	1.9199	4.0000	5.0000	6.0000
GA	1.0084	2.0083	3.0083	0.8811	1.4047	1.9283	4.0083	5.0084	6.0083
IPA	1.0548	2.0548	3.0547	0.9275	1.4511	1.9747	4.0548	5.0548	6.0548
GA-IPA	1.0058	2.0057	3.0058	0.8785	1.4021	1.9257	4.0058	5.0057	6.0058
SA	1.0883	2.0883	3.0884	0.9610	1.4846	2.0082	4.0883	5.0884	6.0883
SA-IPA	1.0810	2.0811	3.0811	0.9537	1.4773	2.0009	4.0810	5.0810	6.0811

convergence rate 93% with MSE 10^{-6} . Similarly, one can see that convergence and MSE of SA algorithm improve when it is hybridized with IPA which has 30% convergence with MSE 10^{-4} . The convergence and MSE of all schemes slightly improve when the number of sensors are increased in the array.

4.2. Case II

In this sub-section, the performance of all five techniques is evaluated for three sources. As shown in Table 5, the actual values are $s_1 = 1$, $s_2 = 2$, $s_3 = 3$, $\theta_1 = 0.6981$ (rad), $\theta_2 = 1.3090$ (rad), $\theta_3 = 2.0944$ (rad), $r_1 = 5\lambda$, $r_2 = 6\lambda$, $r_3 = 7\lambda$. In this case, with the increase of sources (unknown), we faced few local minima due to which the accuracy of all schemes degrade slightly. However, the hybrid GA-IPA proves to be the best among all these techniques even in the presence of local minima. The second best is GA.

Now, the reliability and MSE of all schemes are discussed for three sources. As shown in Table 6, the GA-IPA converges many times and has minimum MSE as compared to the other schemes. It converges 85% with MSE 10^{-5} . The second best is GA which converges 80%

Table 6. MSE and % convergence of three sources for different number of sensors.

No. of Elements	Scheme	MSE	% Convergence	No. of Elements	Scheme	MSE	% Convergence
6	GA	10^{-4}	80	10	GA	10^{-5}	84
	IPA	10^{-3}	25		IPA	10^{-4}	35
	GA-IPA	10^{-5}	85		GA-IPA	10^{-7}	88
	SA	10^{-3}	0		SA	10^{-3}	0
	SA-IPA	10^{-3}	4		SA-IPA	10^{-4}	8
8	GA	10^{-5}	82	12	GA	10^{-6}	85
	IPA	10^{-3}	28		IPA	10^{-4}	36
	GA-IPA	10^{-6}	88		GA-IPA	10^{-7}	90
	SA	10^{-3}	0		SA	10^{-3}	5
	SA-IPA	10^{-3}	5		SA-IPA	10^{-4}	10

Table 7. Amplitude, DOA and range of four sources.

Scheme	s_1	s_2	s_3	s_4	θ_1 (rad)	θ_2 (rad)	θ_3 (rad)	θ_4 (rad)	r_1 (λ)	r_2 (λ)	r_3 (λ)	r_4 (λ)
Actual	1.0000	2.0000	3.0000	4.0000	0.6981	1.3090	2.0944	2.7925	5.0000	6.0000	7.0000	8.0000
GA	1.0183	2.0184	3.0183	4.0183	0.7161	1.3274	2.1127	2.8107	5.0183	6.0183	7.0184	8.0182
IPA	1.0445	2.0446	3.0445	4.0445	0.7427	1.3537	2.1391	2.8371	5.0445	6.0445	7.0445	8.0445
GA-IPA	1.0103	2.0104	3.0102	4.0103	0.7083	1.3194	2.1047	2.8028	5.0103	6.0104	7.0103	8.0103
SA	1.1273	2.1274	3.1272	4.1273	0.8254	1.4362	2.2218	2.9199	5.1273	6.1272	7.1273	8.1274
SA-IPA	1.0232	2.0234	3.0231	4.0235	0.7213	1.3322	2.1176	2.8157	5.0232	6.0232	7.0233	8.0232

with MSE 10^{-4} . The effect of increasing the sensors in the array is also shown due to which the convergence and MSE of all these schemes slightly improve.

4.3. Case III

In this sub-section section, the accuracy of four sources impinging on ULA is discussed. The actual values are considered as $s_1 = 1$, $s_2 = 2$, $s_3 = 3$, $s_3 = 4$, $\theta_1 = 0.6981$ (rad), $\theta_2 = 1.3090$ (rad), $\theta_3 = 2.0944$ (rad), $\theta_4 = 2.7925$ (rad), while $r_1 = 5\lambda$, $r_2 = 6\lambda$, $r_3 = 7\lambda$, $r_4 = 8\lambda$. In this case, we faced even more strong local minima as compared to the previous case. Due to the presence of these strong local minima, the accuracy of all techniques despoiled. GA got stuck little in these local minima which are the inherent ability of GA and its performance improves more when it is hybridized with IP as shown in Table 7.

Now, the reliability (convergence rate) of these techniques is discussed for four sources. Even in this case, the hybrid approach GA-IPA converges many times towards the actual values. It converges

Table 8. MSE and % convergence of four sources for different number of sensors.

No. of Elements	Scheme	MSE	% Convergence	No. of Elements	Scheme	MSE	% Convergence
8	GA	10^{-4}	60	12	GA	10^{-6}	65
	IPA	10^{-3}	4		IPA	10^{-3}	5
	GA-IPA	10^{-5}	70		GA-IPA	10^{-7}	77
	SA	10^{-3}	0		SA	10^{-3}	0
	SA-IPA	10^{-3}	1		SA-IPA	10^{-3}	2
10	GA	10^{-5}	62	14	GA	10^{-7}	70
	IPA	10^{-3}	4		IPA	10^{-3}	6
	GA-IPA	10^{-6}	74		GA-IPA	10^{-8}	80
	SA	10^{-3}	0		SA	10^{-3}	0
	SA-IPA	10^{-4}	1		SA-IPA	10^{-3}	2

70% with MSE 10^{-5} for eight sensors in the ULA. The GA converges 60% with MSE 10^{-4} . However, the performance of IPA, SA-PS and SA is drastically despoiled in the presence of local minima. As shown in Table 8, The IPA alone gets out only four times from these local minima while the SA does not avoid the local minima even for a single time. The effect of increasing elements is also considered due to which GA-IPA, GA and SA-IPA improve slightly. All these techniques failed when the number of sensors in the array is less than the number of sources as it becomes an under-determined problem.

As obvious from the previous discussion, GA-IPA proved to be the best technique as compared to GA, IPA, SA and SA-IPA, so from now onwards our discussion will be limited only to GA-IPA. Now, we discussed the proximity in terms of amplitudes, angular separation and ranges of three sources and eight sensors in the ULA. The actual values of amplitudes, DOAs and ranges for all the below cases are taken as $s_1 = 1$, $s_2 = 3$, $s_3 = 5$, $\theta_1 = 0.5236$ (rad), $\theta_2 = 1.2217$ (rad), $\theta_3 = 2.2969$ (rad), $r_1 = 0.5\lambda$, $r_2 = 4\lambda$, $r_3 = 7\lambda$ respectively. No noise is considered in the system and 10^{-2} is taken as threshold MSE value.

4.4. Case IV

In this sub-section, the behavior of GA-IPA technique is discussed for the amplitudes proximity. Every time, only the values of amplitudes are changed while the values of DOA and ranges are left unchanged. As shown in Table 9, the performance of GA-IPA in terms of accuracy, MSE and convergence rate degrades especially when the amplitudes are very close to each others. However, the GA-IPA is robust enough even to produce fairly good results for proximity of amplitudes.

Table 9. GA-IPA for amplitude proximity.

	s_1	s_2	s_3	θ_1	θ_2	θ_3	r_1	r_2	r_3	MSE	Convergence
Actual Values	1.0000	3.0000	5.0000	0.5236	1.2217	2.2689	0.5000	4.0000	7.0000		
Estimated Values	1.0054	3.0053	5.0054	0.5290	1.2270	2.2743	0.5054	4.0053	7.0053	10^{-6}	89%
Actual Values	1.0000	2.0000	5.0000	0.5236	1.2217	2.2689	0.5000	4.0000	7.0000		
Estimated Values	1.0058	2.0058	5.0054	0.5291	1.2272	2.2744	0.5055	4.0054	7.0053	10^{-6}	88%
Actual Values	1.0000	1.5000	5.0000	0.5236	1.2217	2.2689	0.5000	4.0000	7.0000		
Estimated Values	1.0061	1.5062	5.0057	0.5293	1.2274	2.2745	0.5056	4.0056	7.0055	10^{-6}	86%
Actual Values	1.0000	1.5000	2.0000	0.5236	1.2217	2.2689	0.5000	4.0000	7.0000		
Estimated Values	1.0065	1.5067	2.0067	0.5295	1.2276	2.2747	0.5058	4.0059	7.0057	10^{-5}	84%

Table 10. GA-IPA for DOA proximity.

	s_1	s_2	s_3	θ_1	θ_2	θ_3	r_1	r_2	r_3	MSE	Convergence
Actual Values	1.0000	3.0000	5.0000	0.5236	1.2217	2.2689	0.5000	4.0000	7.0000		
Estimated Values	1.0054	3.0053	5.0054	0.5290	1.2270	2.2743	0.5054	4.0053	7.0053	10^{-6}	89%
Actual Values	1.0000	3.0000	5.0000	0.5236	0.8727	2.2689	0.5000	4.0000	7.0000		
Estimated Values	1.0055	2.0054	5.0055	0.5291	0.8782	2.2744	0.5055	4.0054	7.0054	10^{-6}	88%
Actual Values	1.0000	3.0000	5.0000	0.5236	0.6981	2.2689	0.5000	4.0000	7.0000		
Estimated Values	1.0056	3.0056	5.0057	0.5296	0.7042	2.2747	0.5056	4.0056	7.0055	10^{-6}	85%
Actual Values	1.0000	3.0000	5.0000	0.5236	0.6458	0.7854	0.5000	4.0000	7.0000		
Estimated Values	1.0058	1.5058	2.0059	0.5303	0.6527	0.7924	0.5058	4.0059	7.0057	10^{-5}	83%

4.5. Case V

In this case, the role of GA-IPA is examined for DOA proximity in terms of accuracy, MSE and convergence rate. Each time, only the values of DOAs are changed while keeping the values of amplitude and ranges unchanged. The number of local minima increases, as soon as we brought the DOA close to each other. Due to these local minima the accuracy, MSE and convergence rate degrade, especially when the values of DOA are very close to each others. However, the GA-IPA is still robust enough to produce fairly good results even in this case also as shown in Table 10.

4.6. Case VI

In this sub-section, we examined the proximity of ranges. Each time the values of amplitudes, DOAs are kept same while changing the values of ranges only. Again one can see from Table 11, the performance of GA-IPA affected slightly in terms of accuracy, MSE and convergence when the values of ranges are kept close to each other.

4.7. Case VIII

In this sub-section, the GA-IPA is all together examined for the proximity of amplitudes, DOA and ranges. In this case, more strong local minima arises due to the simultaneous proximity of amplitude, DOA and Ranges. As a result the performance of GA-IPA degrades

Table 11. GA-IPA for range proximity.

	s_1	s_2	s_3	θ_1	θ_2	θ_3	r_1	r_2	r_3	MSE	Convergence
Actual Values	1.0000	3.0000	5.0000	0.5236	1.2217	2.2689	0.5000	4.0000	7.0000		
Estimated Values	1.0054	3.0053	5.0054	0.5290	1.2270	2.2743	0.5054	4.0053	7.0053	10^{-6}	89%
Actual Values	1.0000	3.0000	5.0000	0.5236	1.2217	2.2689	0.5000	2.0000	7.0000		
Estimated Values	1.0055	2.0054	5.0055	0.5292	1.2273	2.2744	0.5059	2.0057	7.0054	10^{-6}	88%
Actual Values	1.0000	3.0000	5.0000	0.5236	1.2217	2.2689	0.5000	2.0000	2.5000		
Estimated Values	1.0056	3.0055	5.0056	0.5293	1.2275	2.2745	0.5061	4.0063	2.5062	10^{-6}	87%
Actual Values	1.0000	3.0000	5.0000	0.5236	1.2217	2.2689	0.3000	0.9000	1.6000		
Estimated Values	1.0057	3.0056	5.0057	0.5295	1.2277	2.2749	0.3070	0.9071	1.6072	10^{-5}	85%

Table 12. GA-IPA for amplitudes, DOA and ranges proximity.

	s_1	s_2	s_3	θ_1 (rad)	θ_2 (rad)	θ_3 (rad)	r_1 (λ)	r_2 (λ)	r_3 (λ)	MSE	Convergence
Actual Values	1.000 0	3.000 0	5.000 0	0.5236	1.2217	2.2689	0.500 0	4.000 0	7.000 0		
Estimated Values	1.005 4	3.005 3	5.005 4	0.5290	1.2270	2.2743	0.505 4	4.005 3	7.005 3	10^{-6}	89%
Actual Values	1.000 0	1.500 0	5.000 0	0.5236	0.6981	2.2689	0.500 0	4.000 0	4.500 0		
Estimated Values	1.006 5	1.506 6	5.005 6	0.5302	0.7049	2.2748	0.506 0	4.006 7	4.006 8	10^{-5}	85%
Actual Values	1.000 0	1.500 0	2.000 0	0.5236	0.6458	0.7854	3.000 0	3.600 0	4.200 0		
Estimated Values	1.008 6	1.508 5	2.008 5	0.5333	0.6565	0.7952	3.008 7	3.608 9	4.208 8	10^{-4}	80%

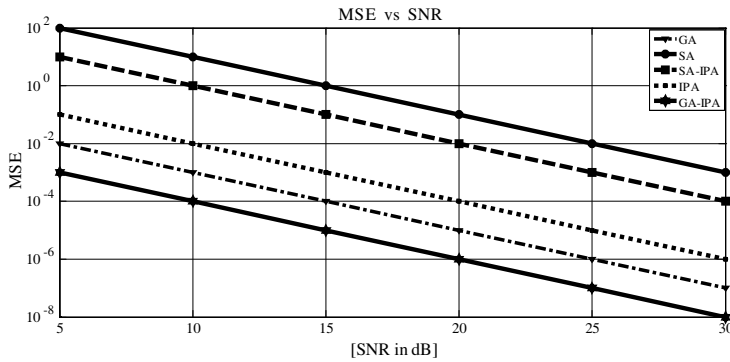


Figure 3. Mean square error vs signal to noise ratio.

more as compared to the previous discussed cases. However, as one can see from Table 12, that even in this case, the GA-IPA acts well to produce fairly good results for the simultaneous proximity of amplitude, DOA and Ranges of three sources.

4.8. Case IX

In this section, we examined the robustness of all schemes against noise. In this case, two sources and eight sensors are considered. The MSE of all five schemes is evaluated against the different values of SNR ranging from 30 dB to 5 dB. As shown in Fig. 3, the hybrid approach GA-IPA is fairly robust even in the presence of low SNR. The second best is GA. Which gives minimum MSE against the different values of SNR.

5. CONCLUSION AND FUTURE WORK

In this work, we propose a method based on memetic computing for the joint estimation of amplitude, DOA and range of near field sources. In this regard, the performance of five techniques have been discussed, i.e., GA, IPA, SA, GA-IPA and SA-IPA. Among these five techniques, the hybrid approach GA-IPA produces fairly better results as compared to GA, IPA, SA and SA-IPA. MSE is used as a fitness evaluation function which is optimum and requires only a single snapshot to converge. All the above mentioned schemes fail when the number of sensors in the array is less than the number of sources. In future, we will use the same approach for three-dimensional arrays.

REFERENCES

1. Bencheikh, M. L. and Y. Wang, "Combined esprit-rootmusic for DOA-DOD estimation in polarimetric bistatic MIMO radar," *Progress In Electromagnetics Research Letters*, Vol. 22, 109–117, 2011.
2. Yang, P., F. Yang, and Z.-P. Nie, "DOA estimation with sub-array divided technique and interporlated esprit algorithm on a cylindrical conformal array antenna," *Progress In Electromagnetics Research*, Vol. 103, 201–216, 2010.
3. Krim, H. and M. Viberg, "Two decades of array processing research: The parametric approach," *IEEE Signal Processing Magazine*, Vol. 13, No. 4, 67–94, July 1996.
4. Liang, J., D. Liu, X. Zeng, W. Wang, J. Zhang, and H. Chen, "Joint azimuth-elevation/(-range) estimation of mixed near-field and far-field sources using two-stage separated steering vector-based algorithm," *Progress In Electromagnetics Research*, Vol. 113, 17–46, 2011.
5. Kim, J. H., I. S. Yang, K. M. Kim, and W. T. Oh, "Passive ranging sonar based on multi-beam towed array," *Proc. IEEE Oceans*, Vol. 3, 1495–1499, September 2000.
6. Ziskind, I. and M. Wax, "Maximum likelihood localization of multiple sources by alternating projection," *IEEE Trans. on Acoust., Speech, Signal Processing*, Vol. 36, No. 10, 1553–1560, 1988.
7. Challa, R. N. and S. Shamsunder, "Higher-order subspace based algorithms for passive localization of near-field sources," *Proceedings of the 29th Asilomar Conference on Signals, and System Computer*, 777–781, Pacific Grove, CA, October 1995.
8. Emmanuele, G., A. M. Karim, and Y. Hua, "A weighted linear

- prediction method for near-Field source localization,” *IEEE Trans. on Signal Process.*, Vol. 10, 2005.
9. Raja, M. A. Z., J. A. Khan, and I. M. Qureshi, “Solution of fractional order system of bagley-torvik equation using evolutionary computational intelligence,” *Mathematical Problems in Engineering*, Vol. 2011, 2011.
 10. Khan, J. A., M. A. Z. Raja, and I. M. Qureshi, “Stochastic computational approach for complex nonlinear ordinary differential equations,” *Chinese Physics Letter*, Vol. 28, 2011.
 11. Zaman, F., I. M. Qureshi, A. Naveed, J. A. Khan, and R. M. A. Zahoor, “Amplitude and directional of arrival estimation: Comparison between different techniques,” *Progress In Electromagnetics Research B*, Vol. 39, 319–335, 2012.
 12. Zaman, F., I. M. Qureshi, A. Naveed, and Z. U. Khan, “Real time direction of arrival estimation in noisy environment using particle swarm optimization with single snapshot,” *Research Journal of Applied Sciences, Engineering and Technology*, Vol. 4, No. 13, 1949–1952, 2012.
 13. Sastry, C. R., E. W. Kamen, and M. Simaan, “An efficient algorithm for tracking the angles of arrival of moving targets,” *IEEE Trans. on Signal Process.*, Vol. 39, No. 1, 242–246, 1991.
 14. Wu, Y. T., Y. Dong, and G. S. Liao, “Jointly estimating both range and doa of near field source,” *Journal of Electronics*, Vol. 21, 104–109, China, 2004.
 15. Dantzig, G. B. and M. N. Thapa, *Linear Programming 2: Theory and Extensions*, Springer-Verlag, 2003.
 16. Forsgren, A., P. E. Gill, and M. H. Wright, “Interior methods for nonlinear optimization,” *SIAM Review*, Vol. 44, 525–597, 2002.
 17. Granville, V., M. Krivanek, and J. Rassin, “Simulated annealing: A proof of convergence,” *IEEE Trans. on Pattern Anal. and Mach. Intell.*, Vol. 16, No. 6, 652–656, 1994.
 18. De Vicente, J., J. Lanchares, and R. Hermida, “Placement by thermodynamic simulated annealing,” *Phys. Lett. A*, Vol. 317, No. 5, 415–423, 2003.
 19. Addad, B., S. Amari, and J.-J. Lesage, “Genetic algorithms for delays evaluation in networked automation systems,” *Engineering Applications of Artificial Intelligence*, Vol. 24, 485–490, Elsevier, 2011.
 20. Maulik, U., “Analysis of gene microarray data in a soft computing framework,” *Engineering Applications of Artificial Intelligence, Elsevier, Signal Process*, Vol. 24, 485–490, 2011.